PAPER

Check for updates

Hydrophobic nano SiO₂ as flow-enhancing additives and flame retardant synergizes with CaCO₃ to suppress gas explosion

Jibiao Xie, [ID] Jiaqi Zhang, Ce Ding and Xiaoli Wang*

The suppression effect of hydrophobic nano SiO₂ of different concentrations as flow-enhancing additives synergizing with CaCO₃ to inhibit gas explosions was systematically studied in a self-built LabVIEW-based explosion test platform. The results showed that the addition of hydrophobic powder can reduce the angle of rest and enhance the flowability of mixed powders, and improve the powder diffusion effect and storability. Meanwhile, changing the proportion and concentration of the mixed powders had a significant impact on the combustion reaction, so that the flame propagation velocity and explosion overpressure decreased significantly. However, excessive powder concentration will promote the combustion reaction at the initial stage of the explosion, and the synergistic inhibition effect of the two powders on explosions is better than that of a single powder. Based on the above results, the optimum suppression concentration and proportion were determined, the mechanism of suppressing gas explosion by a powder was analyzed, and the coupling relationship between flame velocity and pressure was summarized.

1. Introduction

Most coal mines are underground, for which gas explosions are always a threat because of the complicated geological conditions and some man-made factors. Inert gas, water mist, powder, porous materials and aerosols are common gas explosion suppressants and have achieved good performance in actual use. The most effective and common method to ensure safe coal mine working conditions is to use active fire and explosion suppression systems designed to detect and chemically suppress an explosion in its earliest stages. BVS (Germany) and Graviner (U.K.), as well as more advanced developments such as ASVP-LV (Russia) and ExploSpot (South Africa), are extensively used for this purpose. Active methods have found application in the mines of Russia, South Africa, Australia, and China.[1–4] Inert gas and ultrafine water mist can inhibit the explosion through heat absorption, diluting the gas concentration, and interrupting the reaction chain, and porous media can directly lead to the extinction of the flame. In the actual use of active fire and explosion suppression systems, the main components used to inhibit the propagation of the flame are mostly dry powders. Many studies have shown that inert particles such as ABC powder, CaCO₃, Na₂CO₃, and SiO₂ have been used to suppress gas explosions and act to directly reduce the blast pressure,[5–8] and Al(OH)₃, (NH₄)₂SO₄, NaCl, diatomite and bauxite all have a certain inhibitory effect on methane

explosions.[9–11] In an experimental study, inert powder and mixed powders of different ingredients were used as explosion inhibitors to carry out explosion-proof experiments with different-scale experimental tubes and spherical equipment. It was concluded that the influence of various powder inhibitors depends on the explosion limits, pressure, pressure decay rate, flame propagation velocity, velocity decay rate, the coupling relationship between pressure and velocity changes, and some other parameters of the gas, and the explosion of a mixture of gas and coal dust.

Liu's experiments also showed similar results. SiO₂ and CaCO₃ powder can greatly inhibit the explosion overpressure and propagation velocity of a methane–coal dust–air mixture, and ultrafine SiO₂ is more likely to contact and absorb free radicals near the combustion reaction zone, which has the effect of a flame retardant.[12] In addition, a variety of means of synergistic explosion suppression has been proposed, and research has shown that ABC powder and CO₂ can play a very good synergistic role in the suppression of methane explosions.[7] The method of a vacuum chamber and a vacuum chamber in combination with an inert gas has also been proved to be effective in restraining a gas explosion, and study results show that a vacuum chamber can decrease the explosion overpressure and has the effect of absorbing shock waves and energy.[13–16]

The most common device used to inhibit flame propagation is the dry powder fire extinguisher, where the flowability of the powder greatly affects the effectiveness of the fire extinguisher. In recent years, people have become increasingly aware of the impact of high flowability on the protective properties of the

School of Environmental Science and Safety Engineering, Tianjin University of Technology, Tianjin 300384, China. E-mail: xjb603017@163.com; tjutwxl@163.com

particles. The powder is liable to take up moisture during storage (because of the hygroscopic nature of the powder components), and therefore functional additives aid in making the powders more hydrophobic, which is essential to preventing clumping and increasing flowability throughout the life cycle of the powders.[17,18] The flowability of powders with flame retardant or explosive suppression characteristics is influenced by factors including particle size, specific surface area, water content, hydrophobicity, and interparticle forces. These parameters play a positive or negative role in fire and explosion protection. Usually, with a larger particle size, the better is the mobility of the powder, and there will be an increase in powder liquidity for powder diffusion, which plays an important role in fire and explosion prevention, but a lot of research shows that the smaller the particle size of the powder diffusing in the explosive environment, the better the inhibition effect on the explosion. To solve this problem, the selection of appropriate additives for fire suppression and detonation can help improve the existing shortcomings; therefore, the use of flow-enhancing additives in a detonation suppression powder to enhance its storage capacity, diffusion effect, and synergistic detonation research is very important.[19,20]

In recent years, the modification of nano SiO_2 by the hydrothermal method has become more mature. The modified SiO_2 is a superhydrophobic material with low surface energy, and its static contact angle can reach $158.0° \pm 5.4°$, with good hydrophobicity. Functional additives significantly reduce interparticle interaction forces (van der Waals, electrostatic, and capillary). On the one hand, the hydrophobic powder can prevent the powder from agglomerating with moisture, and on the other hand, it can reduce the friction of rough surfaces.[20–22] Studies have been conducted to analyze the effect of different particle sizes of SiO_2 on gas explosions. At this time the micron-sized SiO_2 in the study is only used as a flame retardant, while the modified nano SiO_2 with its hydrophobicity has a greater surface area and hydrophobicity, so the nanometer powder at a certain concentration can reduce the tensile strength to the maximum, but there has been no study on the synergistic explosion suppression effect of this composite property.[23,24] In the present work, we designed an explosion test system based on LabVIEW, and explored the application of hydrophobic nano SiO_2 powder's flowability enhancing effect and flame retardant effect in suppressing explosions. The experiment also analyzed the coupling relationship between velocity and pressure in the explosion and the mechanism of the powder suppressing the explosion. Additionally, the optimum powder concentration and proportion for suppressing a gas explosion are also discussed.

2. Experimental design

2.1 Test platform

The flame propagation behaviors in explosions cannot be clearly studied by conducting experiments in a confined space. Consequently, we designed an open-space explosion experimental apparatus based on LabVIEW and the explosion test container uses a long high-borosilicate toughened glass tube that can withstand a pressure of 2.5 MPa, with a total length of 1000 mm and an inner diameter of 10 mm. The two ends of the long pipe are reinforced with quick-connect flanges and sensors are installed. The outer wall is reinforced with stainless steel and installed with photosensitive sensors, and the long pipe is equipped with 15 photosensitive sensors to record the flame propagation process. The photosensitive sensor model is SGPN88MQ, its spectral response range is 230–1050 nm, and its response time is less than 2 ns. To avoid the photoelectric signal
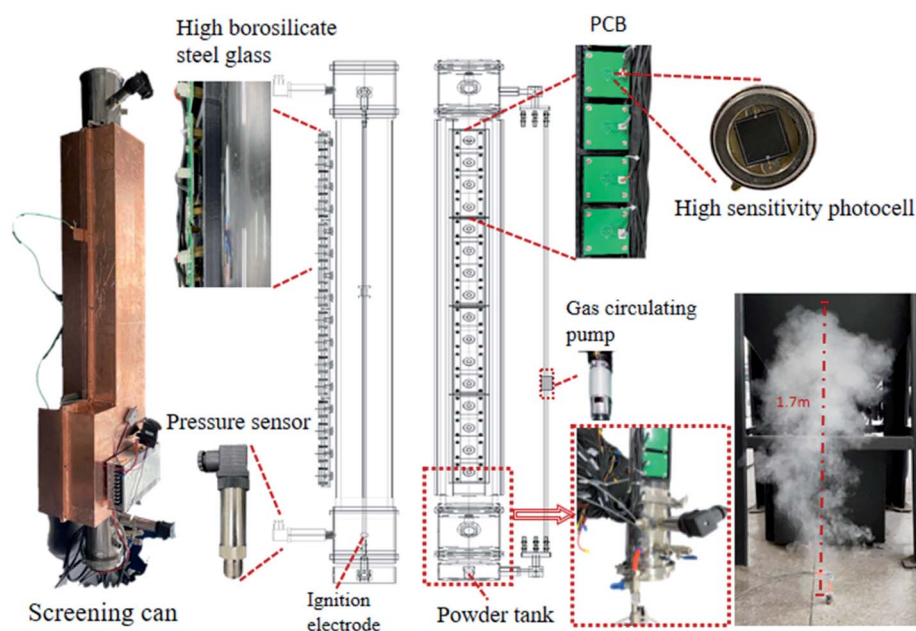

Fig. 1 Explosion experimental apparatus.

interference test caused by the external light source and flame light reflection, each photosensitive sensor is fixed with a black PLA material shading slot to make it accept only the photo-electric signal in the current position tube. The pressure sensor collection range is 0–1 MPa, and the accuracy is 0.5% FS. One of the two pressure sensors is placed at the position of the igniter and the other is placed at the back section of the long pipe. The ignition system consists of a pair of electrodes with a diameter of 2 mm and a high-voltage transformer with capacity of 12 kV to produce sufficient ignition energy. The air inlet and the air outlet at both ends of the long pipe have an interface for connection to the circulating pump, so that the gas in the chamber is evenly mixed, and the circulating pump has a flow rate of 5 L min^{-1}. The powder spraying device uses premixed gas to carry the powder. The test powder is arranged in the tank in advance, and the high-pressure premixed gas is used to spray the dust vertically. The spray pressure is 0.8 MPa and the spray height reaches 1.7 m. The device shell uses black PLA material, which can prevent external light from interfering with the photosensitive sensor. On the other hand, the material is light in weight and strong, and the surface is covered with copper foil to provide a good shielding effect. The experimental apparatus is shown schematically in Fig. 1. All sensors and control components are linked by an NI data acquisition card, and interaction with the computer is realized through LabVIEW programming. The acquisition frequency of the NI data acquisition card is 250 kHz, and the acquisition frequency of the photosensitive sensor of each channel is 15.6 kHz, and the distance between each photoelectric sensor is about 70 mm. With good shielding measures, it can capture photoelectric signals at speeds above 200 m s^{-1} and describe the dynamics of explosion flames in detail. A flow chart of the test platform is shown in Fig. 2.

Design of the system through LabVIEW (Fig. 3). The analog voltage range in the circuit under test is adjusted to −1 to 1 V in the virtual instrument, and functions such as reservation and trigger in the function library are called on to directly collect data and perform underlying operations on the sensor. To determine the virtual instrument layout of the signal on the NI acquisition card according to the flame propagation sequence, the physical channel of DAQ acquisition is used, and the main parameters are set, such as sampling rate, sampling number, filtering parameters, and measurement nodes. The operator processes the operation on the host computer interface through the event structure, and collects, analyzes, and saves the data from the photoelectric and pressure sensor and responds to

events. It then generates the event corresponding to the operation, and then transmits the event response to each module through the queue. In the output signal, digital filtering, amplitude correction, and related operations are implemented together. Finally, after processing the signal, the output can obtain detailed data such as explosion overpressure and flame propagation speed.

2.2 Experimental conditions

This experiment is to investigate the inhibitory effect of nano-hydrophobic powders as flame retardants and flow enhancers synergistically with nano CaCO$_3$ powders on gas explosions. Therefore, the following conditions were considered for the experiment: ① 4.5%/6.5%/9.5%/11% gas–air mixture in volume fraction; ② 9.5% gas–air mixture with a spray powder concentration of 106 g m^{-3}, powder mixed with 30 nm CaCO$_3$ powder, 10 nm/50 nm SiO$_2$ powder (ratios 1 : 0.5/1 : 1/1 : 1.5/1 : 2); ③ 9.5% gas–air mixture, sprayed with SiO$_2$ powder mixed with CaCO$_3$ powder at concentrations of 53, 106, 159, 212 g m^{-3} (ratio 1 : 1). All experimental powders were stored under normal conditions for 5 days. A flow meter was used to control the preset volume fraction of mixed gas in the inlet condition, and the 4-fold volume method was used for gas transmission to ensure the elimination of excess gas in the pipe. After gas transmission is completed, the circulating pump is used for 5 min, and the circulating pump has a flow rate of 5 L min^{-1}. The angle of rest of the powder was measured by the constant-fall method under different conditions, and the combustion products and excess dust were blown off and dried in the explosion pipe after each experiment using a high-flow air pump. The weight of the powder remaining in the powder storage container after completion of the explosion test was obtained by collecting and weighing the residual powder in each storage container. The formula for calculating the spray efficiency of powder in each container is

$$\eta_i = \frac{m_a - m_b}{m_a} \times 100.$$

where m_a is the quantity of powder filling the storage container before the explosion test and m_b is the quantity of powder remaining in the storage container after the explosion test. Therefore, the spray efficiency of the powder is
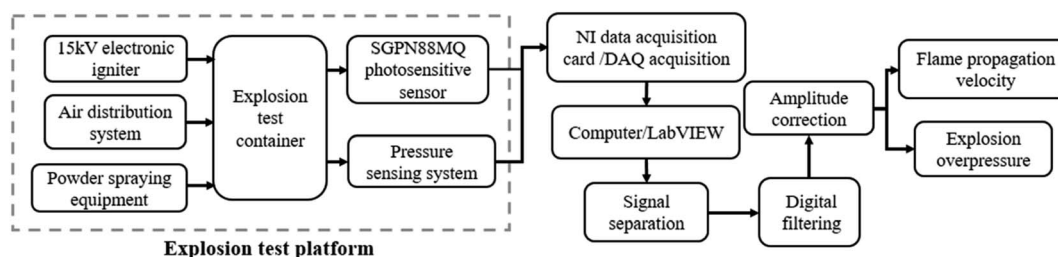
$$\eta = \frac{1}{n} \sum_{i=1}^{n} \eta_i$$
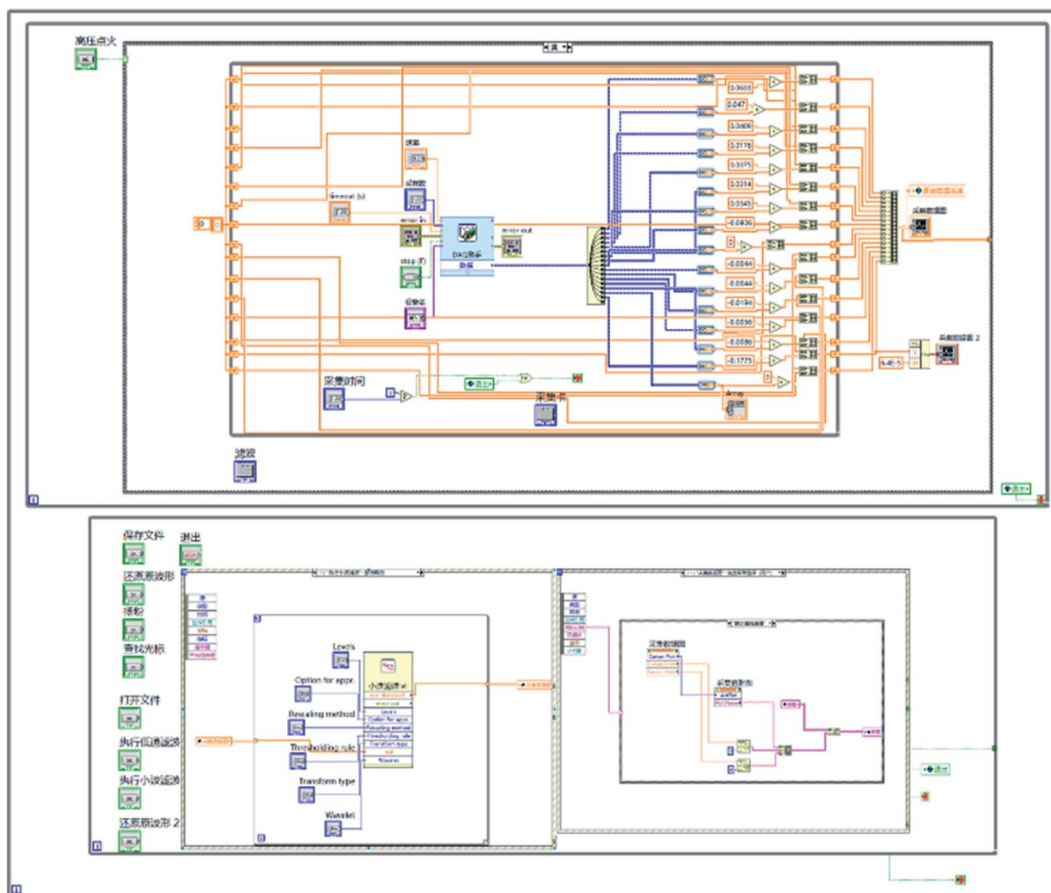

Fig. 2 Test system structure diagram.

Fig. 3 LabVIEW programming diagram.

where n is the number of experiments for each condition. The spray efficiency η is shown in Table 1. All conditions were repeated three to five times, together with separate experiments aimed at achieving reliable and reproducible results. The results show that the addition of hydrophobic powder can reduce η, which proves that the spraying effect of the powder has been improved.

3.   Results and discussions

A gas explosion with a volume fraction of 9.5% is the most violent, and the flame propagation changes more obviously. After the premixed gas is ignited, the flame propagation velocity rises in an oscillating manner under the action of pressure, reaching a maximum value (97.22 m s^{-1}) at the outlet, and the

pressure in the tube rises to the maximum overpressure (17.5 kPa). During the whole process, the average flame propagation velocity is 47.2 m s^{-1}. The experiment uses 9.5% volume fraction methane for the experiment.

3.1   Effect of hydrophobic powder on flame propagation velocity

Table 1 and Fig. 4 give the parameters and images of the mixed powders under different conditions and TEM image of SiO_2. The angle of repose of $CaCO_3$ powder after storage is 51.89°. After adding hydrophobic SiO_2, the angle of repose of the mixed powder after storage can be reduced to 39.59°, and the angle of repose of adding hydrophobic powder is greatly reduced. The difference between 10 nm and 50 nm hydrophobic nano SiO_2 on the powder flowability enhancement effect is not large, and

Table 1   Mixed powder parameters under different working conditions

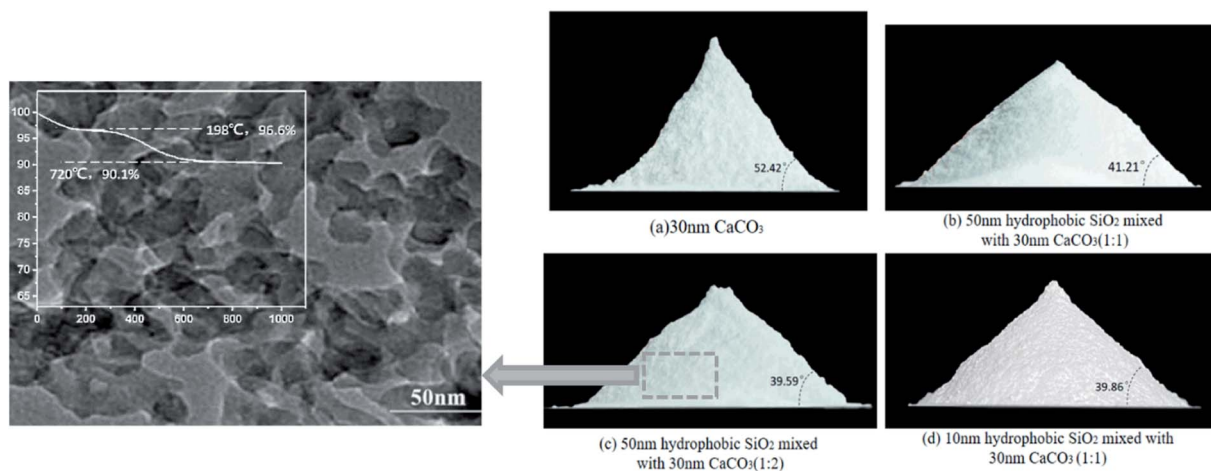| Condition	30 nm CaCO$_3$	50 nm SiO$_2$: 30 nm CaCO$_3$ (1 : 0.5)	50 nm SiO$_2$: 30 nm CaCO$_3$ (1 : 1)	50 nm SiO$_2$: 30 nm CaCO$_3$ (1 : 1.5)	50 nm SiO$_2$: 30 nm CaCO$_3$ (1 : 2)	10 nm SiO$_2$: 30 nm CaCO$_3$ (1 : 1)	10 nm SiO$_2$: 30 nm CaCO$_3$ (1 : 2)
Angle of repose	51.89°	40.58°	39.59°	42.18°	40.25°	39.86°	39.75°
BET (m^2 g^{-1})	21	127	101	84	73	132.5	95.7
η (%)	5.21	4.78	4.68	4.55	4.83	4.97	4.54

Fig. 4 (left) TEM image of SiO$_2$ and TG; (right) angle of repose.

increasing the content of the hydrophobic powder in the mixed powder cannot continue to increase the flowability of the mixed powder. After adding the hydrophobic powder, the spraying efficiency of the mixed powder has also been improved, which proves that the flowability and diffusion effect of the mixed powder have been enhanced, which has positive significance for the storage and spraying of the powder.

Fig. 5 shows the flame propagation velocities under the suppression of mixed powders with different proportions. When no powder is used, the whole reaction process is not hindered, the flame propagation speed of gas explosion rises rapidly, the average propagation velocity of the explosion is 47.1 m s^{-1}, and the maximum value reaches 100.1 m s^{-1} at the outlet. When the concentration is 106 g m^{-3}, the average flame propagation velocity under the inhibition of CaCO$_3$ is 9.26 m s^{-1} with obvious oscillation and it can be seen that the flame propagation velocity can be reduced significantly by using nano CaCO$_3$ powder, but the flame propagation velocity will increase rapidly at the initial stage of the explosion. During the explosion, the decay rates of average velocity and maximum overpressure are 84.7% and 40.4%, as shown in Fig. 6. Meanwhile, using only SiO$_2$ powder can also reduce the flame propagation velocity, and the decay rates of average velocity and maximum overpressure are 79.1% and 47.4%, but the explosion suppression effect after 600 mm in the pipeline is not as good as that of CaCO$_3$. It can be seen from the decay rate results that the
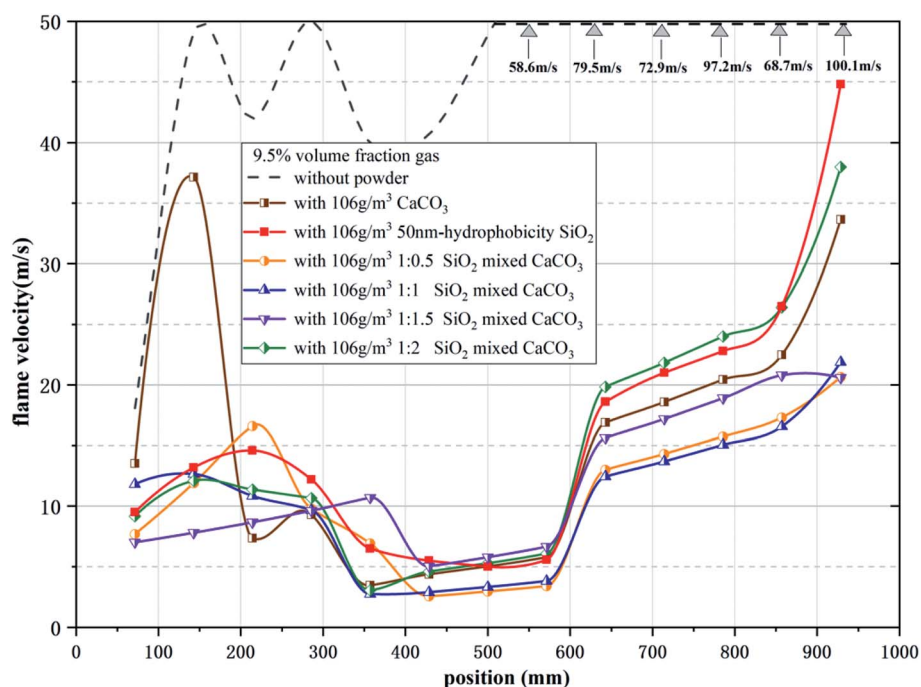

Fig. 5 Flame propagation velocities of different proportions of mixed powder.
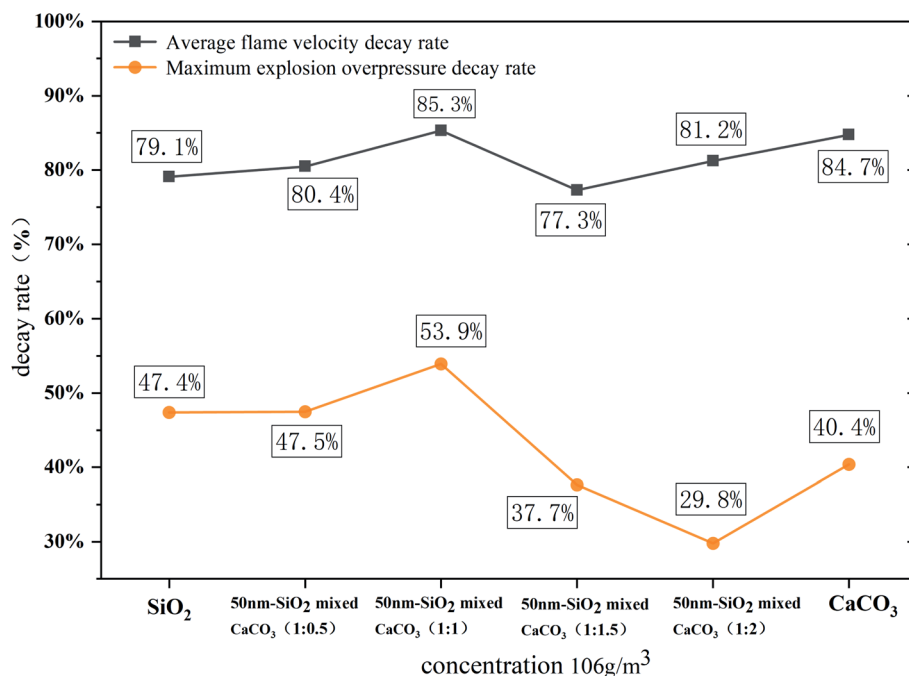
Fig. 6 Decay rate under different working conditions.

group with a higher proportion of SiO_2 in the mixed powder has a better suppression effect on explosion pressure, while the calcium carbonate powder has a weaker suppression effect on explosion pressure, which may be related to the surface structure of powder particles. At the initial stage of the explosion, $CaCO_3$ failed to be pyrolyzed because the flame temperature was still rising gradually, which resulted in a weak ability to inhibit flame propagation at 200 mm in the front section of the long tube. At this time, the flame propagation velocity rapidly increased to its maximum (37.1 m s^{-1}). With the occurrence of pyrolysis, a large number of free radicals in the tube combine, which weakens the explosive chain reaction and hinders the transfer of heat to combustibles, resulting in a decrease in flame propagation velocity. Under the action of pressure, the velocity rises again before reaching the outlet.

The results showed that the explosion was also suppressed in several sets of working conditions with the addition of hydrophobic nano SiO_2. However, increasing the proportion of calcium carbonate or silicon dioxide in the mixed powder does not continue to reduce the flame propagation speed, and the two powders show the best inhibition effect when mixed in a ratio of 1 : 1, which is related to both the diffusion effect of the mixed powder and the chemical properties of the powder itself. The flame propagation velocity shows a greater recovery near the outlet, which is due to the instantaneous release of pressure and heat after the PVC film is broken, and the pyrolysis ability of the flame front to $CaCO_3$ is decreased. At this time, the SiO_2 powder with its relatively large specific surface area plays the main role in inhibition. The curves of the four conditions with the addition of hydrophobic powder show a certain similarity, and they are significantly different from the curves without the addition of hydrophobic powder, especially in the early stage of

the explosion. Because of the modified SiO_2 powder with a large specific surface area, the mixed powder can absorb more precursor shock waves and combine more free radicals at the initial stage of the explosion, so the results show that the flame velocity does not rise as rapidly in the early stages of the explosion as when only $CaCO_3$ powder is used. When nano SiO_2 and $CaCO_3$ were mixed in a one-to-one ratio, the flame propagation velocity was reduced to 2.88m s^{-1} at 400–500 mm. The average flame propagation velocity decay rate reached 85.3%, and the maximum overpressure decay rate reached 53.9%. Both decay rates are the maximum under six working conditions.

3.2 Explosion suppression mechanism

Although hydrophobic SiO_2 can reduce the angle of repose of mixed powder, SEM and EDS layered images show that $CaCO_3$ powder still undergoes agglomeration (Fig. 7 left), and fine SiO_2 powder adheres to the surface of agglomerated $CaCO_3$ to prevent it from further agglomeration. The mixed powder inhibits the combustion reaction in different states of dispersion or agglomeration. Fig. 7 describes the mechanism of explosion inhibition by the mixed powder. Based on the radical chain reaction theory, the gas explosion reaction produces many free radicals, such as [O], [H], [CH$_3$] and [OH]. Owing to the high specific surface area of the nano-powder, especially the modified hydrophobic SiO_2 powder, the fine particles easily contact and absorb free radicals. The SiO_2 powder does not react with the flame, but reduces free radical concentration and reactivity character, which in turn depresses the combustion chain reaction rate, and finally suppresses the explosion flame velocity and overpressure.[25–27] Secondly, it can be seen from thermogravimetry that $CaCO_3$ powder will start to lose a large
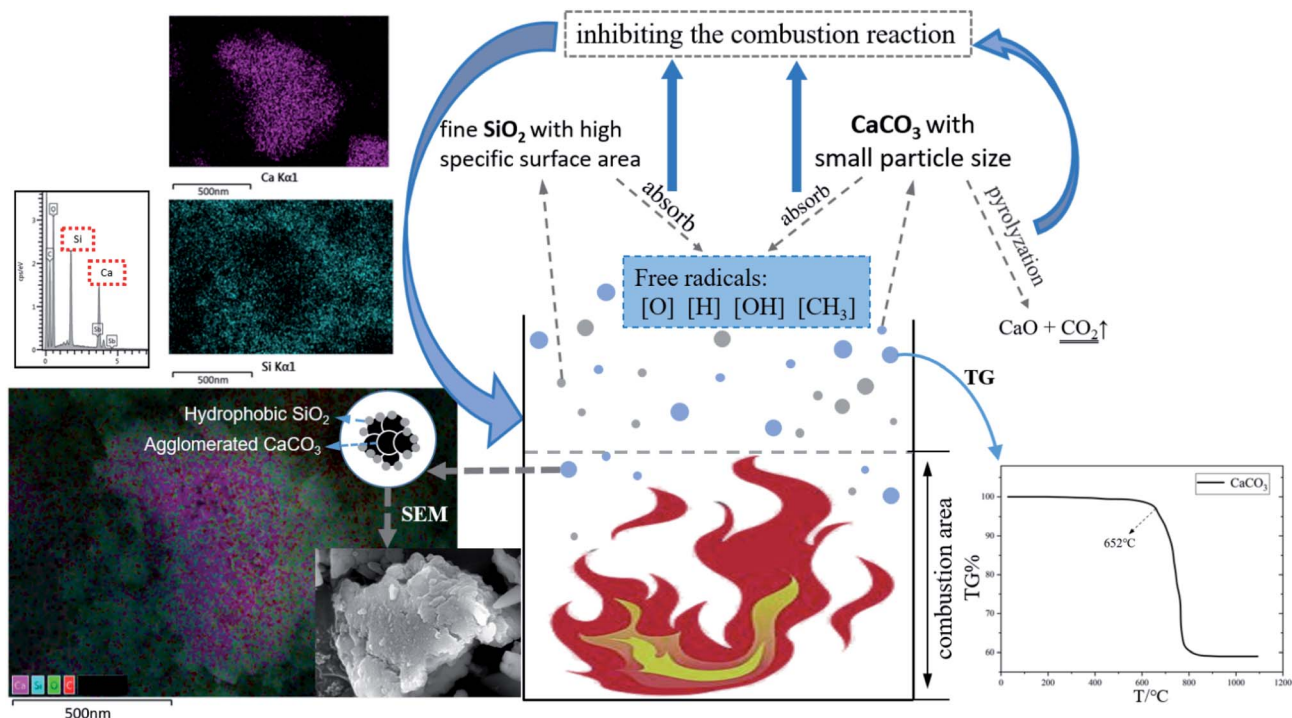
Fig. 7 Suppression mechanism of nano SiO$_2$ and nano CaCO$_3$ (thermogravimetric analysis (TG) image right; energy dispersive spectrometer analysis (EDS layered image) image left).

mass at 652 °C, and the fine CaCO$_3$ particles are more inclined to pyrogenation near the combustion region. Meanwhile, particle size has a great influence on the pyrolysis of CaCO$_3$, and the decomposition rate increases with a decrease in particle size. There are some CaCO$_3$ powders with a smaller particle size distribution, which are easier to pyrolyze in the combustion area, with lower decomposition temperature and a faster decomposition rate, all of which provide the particles with the chance to compound with free radicals in the combustion reaction region, thus reducing the free radical concentration. According to the results in Fig. 6, the suppression of explosions by using CaCO$_3$ only is weak in the front section of the long pipe (up to 200 mm), which may be because CaCO$_3$ has not been pyrolyzed at the beginning of explosion. When mixed powder is used, SEM and EDS stratification diagrams show that fine SiO$_2$ adheres to the surface of agglomerated CaCO$_3$, and external SiO$_2$ reacts first. Fine SiO$_2$ can effectively weaken the chain reaction at the beginning of the explosion by absorbing free radicals, which is a good supplement to suppressing the initial explosion process.

3.3 Effect of powder concentration on flame propagation velocity

Fig. 8 shows the effect of powder concentration on suppressing gas explosions. When the dust concentration is small (53 g m^{-3}), the free radicals consumed by the powder are insufficient, and the flame velocity increases rapidly at the initial stage of the explosion, reaching (32.1 m s^{-1}) at 300 mm. The rates of overpressure and velocity decay are low (18.6% and

83.3%). When the powder concentration is large (159 g m^{-3} and 212 g m^{-3}), although the explosion is suppressed, the decay rate of overpressure and velocity is not as good as for 106 g m^{-3}, which is similar to the results of some powder suppressing explosion research.[28] This is because the nano-hydrophobic SiO$_2$ powder has a small particle size, a large specific surface area and oxygen adsorption content, and has a huge phase interface and interfacial energy with the dispersion medium. This highly dispersed multiphase system is likely to exhibit strong agglomeration characteristics. It is easy to produce a secondary powder with a larger particle size in the gas
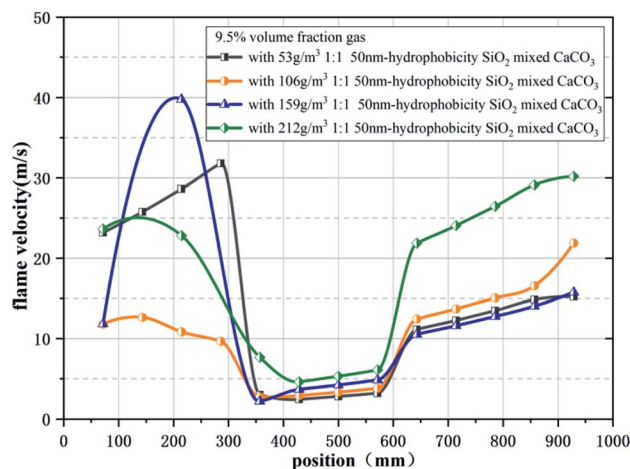

Fig. 8 Flame propagation velocities of different concentrations.

phase.[29–31] When the powder concentration sprayed in the container is increased, the probability of particles colliding with each other increases, and the particles will agglomerate into larger particles, which leads to a decrease in the actual powder concentration and a weakening of the suppression of the explosion. The result of the decay rate in Fig. 9 shows that the influence of powder concentration on explosion pressure is greater than that on flame propagation speed, and too high or too low a powder concentration is not conducive to suppressing the gas explosion. In several sets of working conditions, the mixed powder at 106 g m^{-3} concentration has the best suppression effect on a gas explosion, and the velocity and pressure decay rate are 85.3% and 53.9%, respectively.

3.4 Coupling relationship between flame and overpressure

Fig. 10 shows the coupling relationship between explosion velocity and pressure when SiO_2 and $CaCO_3$ are mixed in a 1 : 1 ratio at a concentration of 106 g m^{-3}. When the igniter ignites the gas, the flame propagation velocity rises rapidly up to 25 ms, but due to the small combustion area in the early stage of flame development, the pressure does not change significantly at this time. At 25–60 ms, the flame propagation velocity decreases continuously, and the absorption of free radicals by the SiO_2 surface is the main inhibitor of the explosion. However, as the combustion reaction continues, the heat generation in the tube is greater than the dissipation, and the pressure gradually rises to 3.5 kPa. At 68 ms, there is a very obvious coupling relationship between velocity and pressure. At this time, the PVC film at the outlet is destroyed, and some heat and gas in the tube are released instantaneously, which leads to a pressure drop in the tube. After the flame front in the combustion zone loses the front pressure, the velocity rises again. After the pressure dropped to 1.8 kPa, affected by the destruction of the PVC film, the flame propagation velocity and explosion pressure showed a similar upward trend within 77–120 ms. On the one hand, when the film is destroyed, the gas carries a large amount of powder out, which reduces the density of unburned gas and the concentration of flame retardant powder. On the other hand,
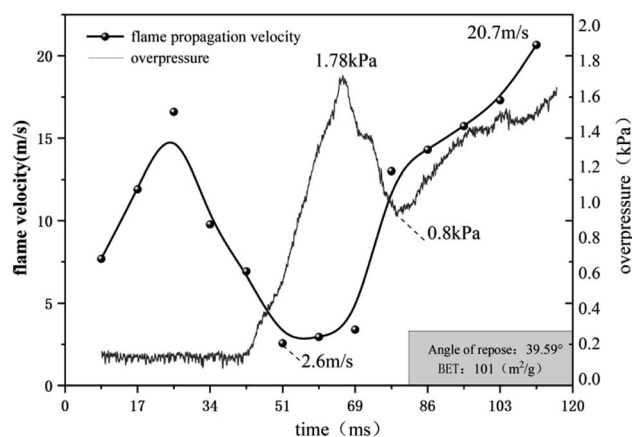

Fig. 10 Coupling relationship between flame and overpressure of mixed powder.

the combustion reaction is still continuing, and the combustion area is also increasing, but the severity of the reaction is decreased. Therefore, although the explosion was suppressed by the powder, the combustion reaction could not be terminated, and the flame velocity and pressure still increased at a small rate.[32]

4. Conclusion

In this paper, the explosion suppression effect of hydrophobic powder was tested by a self-designed LabVIEW-based platform. Nano-hydrophobic SiO_2 powder and nano $CaCO_3$ powder can absorb and consume free radicals in the combustion region, and the modified SiO_2 powder has a larger specific surface area and can easily bind to free radicals, while nano $CaCO_3$ pyrolysis also consumes free radicals, which both inhibits the combustion process and hinders the explosion shock wave. In addition, nano SiO_2 compensates for the weak inhibition of $CaCO_3$ on the combustion reaction at the initial stage of the explosion, and the synergistic effect of the two powders on inhibiting the gas explosion is better than that of a single powder. The flowability of the mixed powder was analyzed after long storage, and the difference in improving flowability between different contents of hydrophobic powder additives was not large, with the maximum decrease in the rest angle of the mixed powder being 10.87°. Under the action of nano-hydrophobic SiO_2 powder, the storability and diffusion effect of the mixed powder were improved. In the process of the explosion, the mixed powder reduces the combustion reaction rate, destroys the positive feedback mechanism, and greatly reduces the flame propagation velocity and overpressure. The six powder concentrations of the experimental species can inhibit the explosion, but too large or too small a powder concentration may weaken the suppression effect. When the dust concentration exceeds a certain range, the explosion suppression effect is not good. The coupled analysis of velocity and pressure changes shows that under suppression by powder, the trends of flame velocity and pressure changes with time are similar, but the pressure change has a certain lag. Meanwhile, the instantaneous change
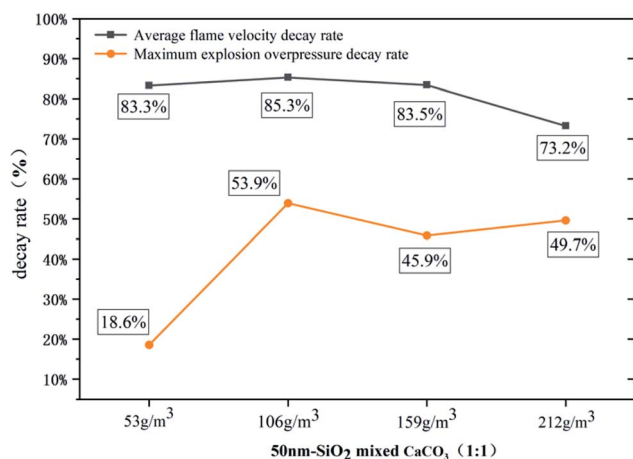

Fig. 9 Decay rate under different working conditions.

in the explosion pressure in the tube will also affect the flame propagation velocity, so the flame velocity can only reflect the strength of the reaction in the combustion area to a certain extent. In this study, when the concentration is 106 g m^{-3}, hydrophobic SiO_2 powder is used as a flow-enhancing additive and flame retardant, and when mixed with nano $CaCO_3$ powder at a ratio of 1 : 1, the synergistic suppression effect on a 9.5% gas explosion is the best. The decay rates of flame propagation velocity and overpressure were 85.3% and 53.9%.

Project fund

Conflicts of interest

There are no conflicts to declare.

References

1 J. J. L. d. Plessis, Active explosion barrier performance against methane and coal dust explosions, *Int. J. Coal Sci. Technol.*, 2015, 268.

2 J. Cheng, *Explosions in Underground Coal Mines Risk Assessment and Control*, Springer International Publishing AG, Part of Springer Nature, 2018, pp. 1–208.

3 B. Nika, C. Nikoloz, M. Edgar, A. Irakli, and C. Mikheil, New Suppression System of Methane Explosion in Coal Mines, *Procedia Earth & Planetary Science*, 2015.

4 Y. Gorlov, ASVPLV.1M automatic methane and dust explosion control and isolation system, *Mining Ind. J*, 2013, **6**, 41–42.

5 G. U. Bao-Shan, H. Y. Wen, Y. T. Liang and X. Y. Wang, Mechanism characteristics of CO2 and N2 inhibiting methane explosions in coal mine roadways, *J. China Coal Soc.*, 2013, **38**(366), 361–366.

6 O. T. Y. Akira, E. Wataru and N. Hiroyoshi, Experimental and numerical investigation of flame speed retardation by water mist, *Combust. Flame*, 2015, **162**, 1772–1777.

7 L. Zhenmin, W. Tao, T. Zhihui, C. Fangming and D. Jun, Experimental study on the suppression of gas explosion using the gas–solid suppressant of CO2/ABC powder, *J. Loss Prev. Process. Ind.*, 2014, **30**, 17–23.

8 Y. Wang, Y. S. Cheng, M. G. Yu, Y. Li, J. L. Cao, L. G. Zheng and H. W. Yi, Methane explosion suppression characteristics based on the NaHCO3/red-mud composite powders with core-shell structure, *J. Hazard Mater.*, 2017, **335**, 84–91.

9 Z. M. Luo, F. M. Cheng, T. Wang, J. Deng and C. M. Shu, Suppressive Effects of Silicon Dioxide and Diatomite Powder Aerosols on Coal Mine Gas Explosions in Highlands, *Aerosol Air Qual. Res.*, 2016, **16**, 2119–2128.

10 Z. Yue, Z. Jing-Lin, Z. Bao-Min and W. Jing-Jing, A Study on Explosion Suppression Effect of No. 92 Gasoline Vapor-air Mixture Using ABC and BC Dry Powders, *China Saf. Sci. J.*, 2013, **23**, 53–58.

11 D. Huang, X. Wang and J. Yang, Influence of Particle Size and Heating Rate on Decomposition of BC Dry Chemical Fire Extinguishing Powders, *Part. Sci. Technol.*, 2015, 488–493.

12 Q. Liu, Y. Hu, C. Bai and M. Chen, Methane/coal dust/air explosions and their suppression by solid particle suppressing agents in a large-scale experimental tube, *J. Loss Prev. Process. Ind.*, 2013, **26**, 310–316.

13 W. Zheng-Yan, J. Shu-Guang, W. Lan-Yun, S. Hao, W. Kai, Z. Wei-Qing, W. Hai-Wei and L. Wei-Wei, Experimental study on explosion suppression of vacuum chambers with different scales, *Procedia Earth Planet. Sci.*, 2009, **1**, 396–401.

14 Z. Wu, S. Jiang, H. Shao, K. Wang, X. Ju, W. Zou, W. Zhang and L. Wang, Experimental study on the feasibility of explosion suppression by vacuum chambers, *Saf. Sci.*, 2012, **50**, 660–667.

15 C. Cui, H. Shao, S. Jiang and X. Zhang, Experimental study on gas explosion suppression by coupling CO2 to a vacuum chamber, *Powder Technol.*, 2018, **335**, 42–53.

16 X. Wen, T. Su, F. Wang, H. Deng, K. Zheng and B. Pei, Inert nanoparticle suppression of gas explosion in the presence of obstacles, *RSC Adv.*, 2018, **8**, 39120–39125.

17 K. Meyer and I. Zimmermann, Effect of glidants in binary powder mixtures, *Powder Technol.*, 2004, **139**, 40–54.

18 O. A. Odeku, S. Weber and I. Zimmermann, Efficiency of Nanoscaled Flow Regulators, *Chem. Eng. Technol.*, 2011, **34**, 69–74.

19 J. Tomas and S. Kleinschmidt, Improvement of Flowability of Fine Cohesive Powders by Flow Additives, *Chem. Eng. Technol.*, 2010, **32**, 1470–1483.

20 Q. Huang, *Improving Fluidizability of Cohesive Particles by Surface Coating with Flow Conditioners*, 2006.

21 J. M. Valverde, A. Castellanos, A. Ramos and P. K. Watson, Avalanches in fine, cohesive powders, *Phys. Rev. E: Stat. Phys., Plasmas, Fluids, Relat. Interdiscip. Top.*, 2000, **62**, 6851–6860.

22 J. L. Anthony, Influence of particle characteristics on granular friction, *J. Geophys. Res.: Solid Earth*, 2005, **110**, B08409.

23 R. J. Gao, Y. Yao, H. Wu and L. Wang, Effect of amphoteric dispersant on the dispersion properties of nanoSiO2 particles, *J. Appl. Polym. Sci.*, 2017, **134**(29), 45075.

24 T. Meng, H. Yu, S. Lian, and R. Meng, *Effect of nanoSiO$_2$ on properties and microstructure of polymer modified cementitious materials at different temperatures, Structural Concrete*, 2020.

25 W. Shimao, D. U. Yang, L. I. Guoqing, Q. I. Sheng, W. Bo and L. I. Yangchao, Overpressure transients and flame behaviors of gasoline-air mixture deflagration in confined space with local opening, *CIESC J.*, 2017, **68**(8), 3310–3318.

26 X. Chen, Y. Zhang, Q. Zhang, *et al.* Experimental investigation on micro-dynamic behavior of gas explosion suppression with SiO2 fine powders[J], *Theor. Appl. Mech. Lett.*, 2011, **1**(3), 032004.

27 H. Wen, Q. H. Wang, J. Deng and Z. M. Luo, Effect of the concentration of Al(OH)3 ultrafine powder on the pressure of methane explosion, *J. China Coal Soc.*, 2009, **34**, 1479–1482.

28 Q. Wang, H. Wen, *et al.* Inhibiting effect of Al(OH)3 and Mg(OH)2 dust on the explosions of methane-air mixtures in closed vessel[J], *Sci. China*, 2012, **55**(5), 1371–1375.

29 S. M. Rolova and B. E. Gel'Fand, Shockwave attenuation in gas suspensions [J], *Combust. Explos. Shock Waves*, 1991, **27**(1), 124–129.

30 M. Sommerfeld, The unsteadiness of shock waves propagating through gas-particle mixtures [J], *Exp. Fluid*, 1985, **3**(4), 197–206.

31 M. Olim, G. Ben-Dor, M. Mond, *et al.* A general attenuation law of moderate planar shock waves propagating into dusty gases with relatively high loading ratios of solid particles[J], *Fluid Dyn. Res.*, 1990, **6**(3–4), 185–199.

32 Z. Ligang, W. Yalei, Y. U. Shuijun, Z. Xiaochao, L. I. Gang, D. U. Depeng and D. Zengguo, Coupled relationship between flame and overpressure of gas explosion inhibited by NaHCO$_3$, *CIESC J.*, 2018, **69**(9), 4129–4136.